

# Highly homogeneous YBCO/LSMO nanowires for photo-response experiments

R Arpaia<sup>1,2</sup>, M Ejrnaes<sup>2,3</sup>, L Parlato<sup>2</sup>, R Cristiano<sup>2,3</sup>, M Arzeo<sup>1</sup>,  
T Bauch<sup>1</sup>, S Nawaz<sup>1</sup>, F Tafuri<sup>4</sup>, G P Pepe<sup>2</sup> and F Lombardi<sup>1</sup>

<sup>1</sup> Quantum Device Physics Laboratory, Department of Microtechnology and Nanoscience, Chalmers University of Technology, S-41296 Göteborg, Sweden

<sup>2</sup> CNR-SPIN, Dipartimento di Scienze Fisiche, Università degli Studi di Napoli “Federico II”, I-80125 Napoli, Italy

<sup>3</sup> CNR-SPIN, Istituto di Cibernetica E. Caianiello, I-80078 Pozzuoli, Italy

<sup>4</sup> Dipartimento di Ingegneria Industriale e dell’Informazione, Seconda Università di Napoli, I-81031 Aversa (CE), Italy

E-mail: arpaia@chalmers.se

**Abstract.** By using nanolithography and a soft etching procedure, we have realized  $\text{YBa}_2\text{Cu}_3\text{O}_{7-x}/\text{La}_{0.7}\text{Sr}_{0.3}\text{MnO}_3$  (YBCO/LSMO) nanowires, with cross sections down to  $100 \times 50 \text{ nm}^2$  that ensures covering areas up to  $10 \times 30 \mu\text{m}^2$ . The LSMO layer acts as a capping for YBCO, minimizing the degradation of its superconducting properties taking place during the patterning; moreover, as a ferromagnetic manganite, it’s expected to accelerate the relaxation dynamics of quasiparticles in YBCO, making such a system potentially attractive for applications in the superconducting ultrafast optoelectronics. The reproducibility of the values of the critical current densities measured in different devices with the same geometry makes our nanowires ideal candidates for photo-response experiments. First measurements have shown a satisfactory photoresponse from YBCO/LSMO devices.

## 1. Introduction

During the last decade the research on nanowires based superconducting photodetectors has gained an increasing interest. Much of the efforts have focused on superconducting nanowires for single photon detection (SNSPD) [1, 2]. Indeed the theoretical performances of these devices in terms of detection efficiencies (close to 100% up to the near infrared wavelength region), together with the extremely low dark counts ( $< 1 \text{ s}^{-1}$ ), fast time response (few ps) and low time jitters ( $< 30 \text{ ps}$ ) [2], are attractive for applications.

Low temperature superconductors (LTS) such as NbN, NbTiN, and more recently WSi have been widely used to fabricate nanowire-based photon detectors [1, 3, 4]. Attention is also devoted to explore the potentialities of unconventional superconductors such as  $\text{MgB}_2$  and  $\text{YBa}_2\text{Cu}_3\text{O}_{7-x}$  (YBCO) [5, 6]. High critical temperature superconductors (HTS), characterized by fast thermalization dynamics, are

*Highly homogeneous YBCO/LSMO nanowires for photo-response experiments* 2

in principle very interesting for realizing nanosized structures useful for photodetection. Unfortunately, serious degradations of the superconducting properties are observed for dimensions approaching the nanometer scale, due to damages/oxygen out-diffusion related to the nanopatterning procedure [7, 8, 9, 10]. In order to reduce these damages a protective layer is typically used and particularly good results have been obtained using gold that allowed the fabrication of nanowires with superconducting properties close to the as-grown film and critical current densities approaching the depairing limit [11, 12].

However, gold is not a good choice for single photon detectors applications. Its high conductivity leads to a high reflection of the light. At the same time, the Au capping layer works as an electrical shunt for the photoresponse and as a thermal shunt for the perturbed area inside the detector. For this reason new protective materials have to be investigated to preserve the properties of the YBCO nanowires during the patterning process.

In this context it is also interesting to investigate functional protective layers, i.e. materials that can positively affect important material properties of the underlying YBCO without deteriorating the detector operation. For this reason superconducting bilayers of YBCO/manganite have been investigated, that in the case of  $\text{La}_{0.7}\text{Sr}_{0.3}\text{MnO}_3$  (LSMO) and  $\text{La}_{0.7}\text{Ca}_{0.3}\text{MnO}_3$  (LCMO) have been reported to be compatible with YBCO both chemically and structurally [13]. Indeed, no significant reduction of both  $T_C$  and  $J_c$ , by proximity effect, has been observed in YBCO/LSMO bilayers [14]. Moreover, nonequilibrium experiments by pump-and-probe fast optical transient reflectivity spectroscopy on several tens of nanometers thick YBCO/LSMO bilayers have demonstrated that LSMO is functionally affecting the underlying YBCO by reducing the electronic relaxation times [15] when compared to bare YBCO films.

On the other hand, the physics of ferromagnet (F)/superconductor (S) heterostructures has attracted a considerable attention during the last decade [16], also in the context of novel solutions for superconducting nanowire detectors [17]. In particular, the interplay between ferromagnetism and superconductivity in cuprate/manganite-oxide heterostructures [18, 19, 20] gives rise to an unexpected long-range proximity effect [21] and to an active and intriguing role of spin diffusion mechanisms at the interface [22]. All these physical characteristics make these nanostructured bilayers quite interesting on the roadmap leading to advanced spintronics devices or possible artificially engineered, ultrafast optoelectronics devices.

In this paper, we present fabrication, transport characterization and preliminary photoresponse measurements of epitaxial YBCO/LSMO nanowires. The presence of the protecting LSMO capping layer guarantees the degree of homogeneity required in order to implement these nanowires in complex configurations, covering very large areas, suitable for photodetection applications.

## 2. Film growth and characterization

A 50 nm thin film of YBCO has been deposited by Pulsed Laser Deposition (PLD) on a (001) LAO substrate, at a  $O_2$  pressure of 0.6 mbar and deposition temperature of  $800^\circ\text{C}$ . These deposition conditions give very smooth surfaces (2 nm roughness) at the expenses of the superconducting properties. To improve the transport properties, soon after the deposition, the film has been heated up to  $865^\circ\text{C}$ , then cooled down in  $O_2$  pressure at 800 mbar at a rate of  $60^\circ\text{C}/\text{h}$ . The resulting film has excellent structural and transport properties, with  $\sim 0.3^\circ$  full width at half maximum rocking curves of the (005) reflection and a sharp superconducting transition (with  $T_C$  of about 89 K) (see Fig. 1). On top of the YBCO layer a 15 nm thin LSMO film has been deposited ex-

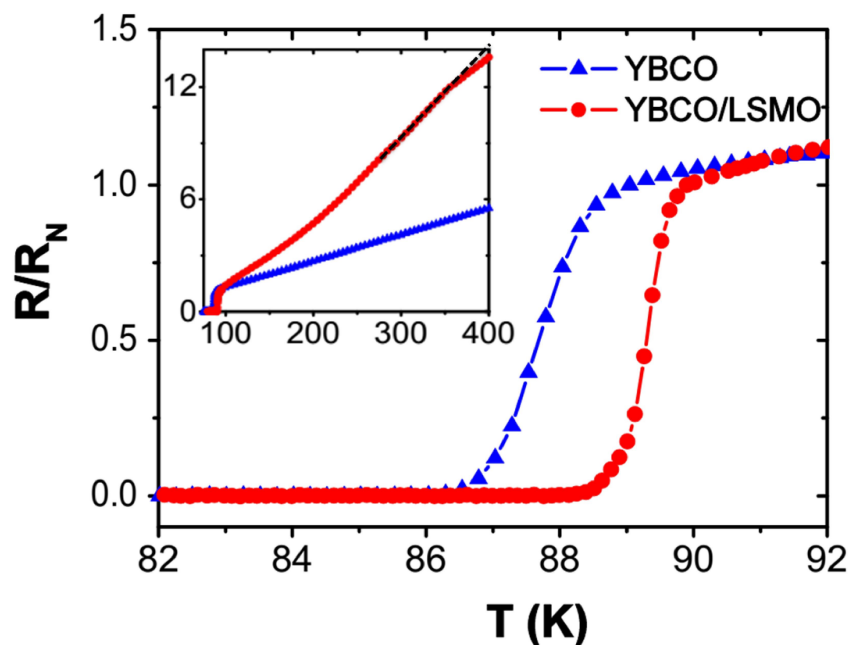


**Figure 1.** Resistance vs temperature (normalized to the normal resistance  $R_N$  at the transition temperature) of a 50 nm thick YBCO film before (*blue triangles*) and after (*red dots*) the deposition of the 15 nm thick LSMO capping layer. The  $T_C$  is enhanced after the deposition of the ferromagnetic layer. As a first approximation, the resistance of the bilayer can be explained in terms of the parallel between the resistance of YBCO and that of LSMO: since the current mostly flows across the YBCO layer that has the lower resistance, the characteristic bump of the metal-insulator transition of LSMO is reduced. However, it's still possible to extract the  $T_{Curie}$  from the bending of the  $R(T)$  at  $T \sim 355$  K, highlighted by the dashed line showed in the inset.

situ by PLD, at 0.2 mbar  $O_2$  pressure and at a temperature of  $730^\circ\text{C}$ . Here, the growth conditions have been optimized to get the right compromise between surface smoothness and Curie temperature  $T_{Curie}$ . Post-annealing of the bilayers at 800 mbar of  $O_2$  has been employed to promote full oxidation of YBCO through the LSMO capping. The final YBCO/LSMO bilayer has a surface roughness smaller than 2 nm and a  $T_C \sim 90$  K,

*Highly homogeneous YBCO/LSMO nanowires for photo-response experiments* 4

with a rather sharp transition with a width below 1 K (Fig. 1). The enhancement of the  $T_C$  in the bilayer, with respect to the single YBCO film is quite surprising, considering that in literature a diminishing  $T_C$  has been reported, and attributed to a suppression of the superconducting properties induced by diffusion of spin-polarized quasiparticles or F/S proximity effect [22, 23]. However, these effects are strongly dependent on the length scales and become dominant if the YBCO layer is very thin ( $\sim 10$  nanometers): in our case instead only an interface effect between the two layers can be considered, inducing a small variation in the oxygen content of YBCO toward the optimal value [24]. Moreover, by measuring the resistance vs temperature dependence, we have obtained that the  $T_{Curie}$  of LSMO is of  $\sim 355$  K, slightly lower than the optimal value reported for the bulk (see inset Fig. 1).<sup>‡</sup> The sheet resistances  $R_{\square}$  at 100 K were measured to be:  $15 \Omega$  for YBCO and  $12 \Omega$  for YBCO/LSMO.

### 3. Design of the devices

For the patterning of the nanostructures, we have followed the same procedure as reported in [11, 12, 25]. In order to use the nanowires for novel photodetection experiments, there is the need for a large area coverage for many applications. As a consequence, several microns long nanowires need to be engineered. In order to make large area devices with narrow wires, different geometries have been previously employed [26, 27, 28]. In this work we have chosen the *parallel configuration*, first proposed in [26] for realizing a *cascade switch mechanism* in NbN SNSPD. It consists of a serial connection of blocks, each formed by nanowires in parallel. The performance of such device, in terms of signal amplitude, is related to the capability to fabricate stripes with very high critical current densities. But the degree of homogeneity of the stripes is even more essential, because the photoresponse is most effective when the stripes are biased around their maximum critical current. The serial connection of blocks of parallel nanostripes also reduces the detrimental effect of single strip defects. This last point is rather crucial for YBCO, where its chemical instability, mostly related to oxygen out diffusion, and its extreme sensitivity to defects make the realization of nanowires with highly homogeneous superconducting properties very challenging.

### 4. Nanopatterning procedure

A 50 nm thick Au film has been deposited by e-beam evaporation on the top of the bilayer YBCO/LSMO. This layer acts as a capping, protecting the structure from damages occurring during the fabrication steps. For the definition of the YBCO/LSMO

<sup>‡</sup> One of the most remarkable properties of LSMO is the strong influence of the magnetic transition on the electronic conduction, induced by the *double exchange* interaction: a transition occurs from the high temperature paramagnetic, highly resistive phase to the low temperature ferromagnetic metallic phase. So, at temperatures above  $T_{Curie}$  it is a bad conductor and  $d\rho/dT < 0$ , while below  $T_{Curie}$   $d\rho/dT > 0$ : the resistance has therefore its maximum around  $T_{Curie}$ .

nanostructures we have used a 100 nm thick carbon film working as a hard mask [7] together with electron beam lithography and  $Ar^+$  ions etching (details of all the fabrication steps can be found in [25]). The main difference with respect to the previous procedures [11, 12, 25] is given by the ion milling etching due to the presence of the additional LSMO layer. As beam parameters, we have chosen to work very close to the etching threshold for YBCO and LSMO so to minimize the interaction of the  $Ar^+$  ions with the nanostructures [11].

The protecting Au is removed by a final  $Ar^+$  ion milling etching. During the etching, LSMO acts as a cap layer for YBCO, preventing the milling species from vertically impinging on the top surface of the nanowires, causing a degradation of the superconducting properties (see Fig. 2a).

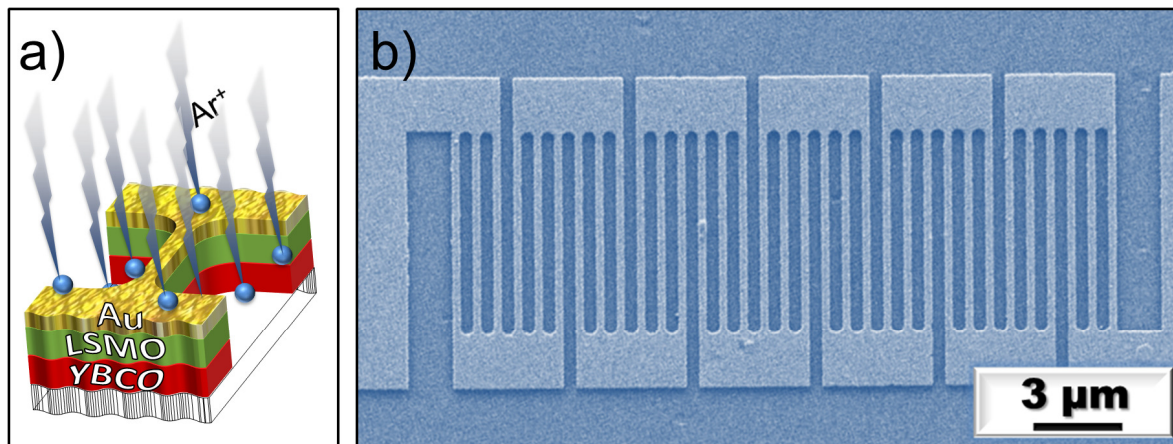


**Figure 2.** a) Schematic of the crucial role LSMO has during the patterning of nanowires: it protects YBCO during the final  $Ar^+$  ion etching of the Au cap. b) SEM picture of a device, made with 300 nm wide YBCO/LSMO nanowires.

We have fabricated YBCO/LSMO nanowires, embedded in 7, 9, 11 and 13 blocks of 3 parallel wires. The wires are up to 10  $\mu\text{m}$  long, with widths ranging between 100 and 300 nm (see Fig. 2b). In this way, we've been able to cover areas up to 10x30  $\mu\text{m}^2$  with a filling factor of 40%.

## 5. Transport characterization of nanowires

To probe the quality and the degree of homogeneity of our YBCO/LSMO nanowires, we have extracted their critical current densities from the current-voltage characteristics (IVCs) measured on different devices both before and after the etching of the Au layer (see Fig. 3a). Moreover we have compared these values with the ones extracted by devices with the same geometries, but without the LSMO layer, in order to check its effective role (see Fig. 3b).

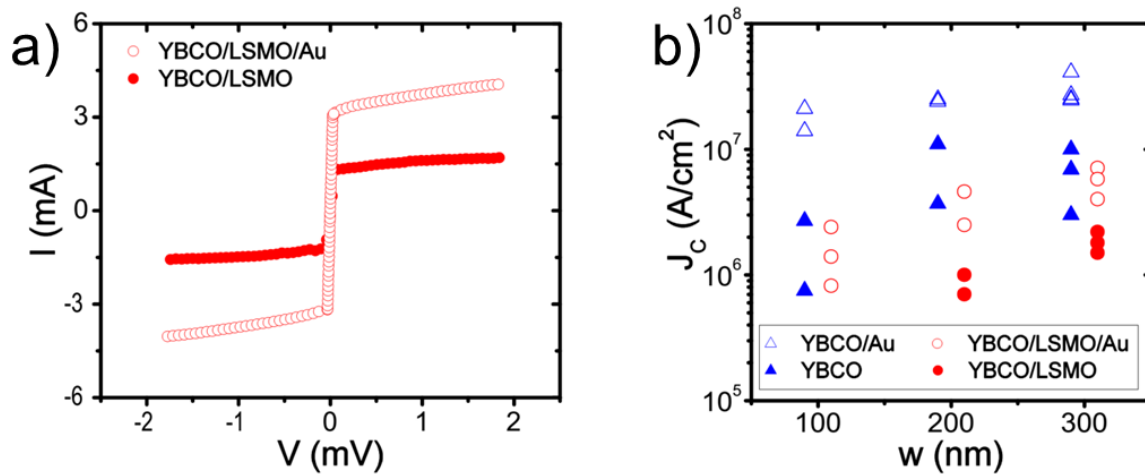


**Figure 3.** a) Flux-flux like IV characteristics of a device made of 300 nm wide YBCO/LSMO nanowires before and after the removal of the gold capping. b) The critical current densities of the YBCO/LSMO (*circles*) and YBCO (*triangles*) nanowires, extracted from different devices, are shown for three different widths (100, 200 and 300 nm), both before (*blue*) and after (*red*) the Au etching. For a better readability, the data sets belonging to YBCO (YBCO/LSMO) have been shifted to the left (right).

Before the Au etching, the transport properties of the YBCO and YBCO/LSMO devices have been obtained by conventional four point measurement at  $T = 4.2$  K. While  $J_c(w)$  of bare YBCO nanowires follows the same behavior already observed in our previous works [11, 12], with rather high critical current densities, independently of the wire width, the extracted critical current densities of YBCO/LSMO nanowires are one order of magnitude lower (Fig. 3b). This significant decrease could be associated to the F/S proximity effect or to the Sr contamination of the superconducting layer [14, 29], possibly enhanced by the reduced dimensions of the YBCO nanowires. However, for wires 200 and 300 nm wide, the measured critical current densities are almost width independent and the spread of values among devices with the same geometry quite limited.

After the Au capping is completely etched, the fundamental role of the LSMO layer becomes clear. Although the etching process has been calibrated so as only a thickness between 2 and 5 nm is removed from the top of the nanostructures, in the case of bare YBCO nanowires the critical current densities are severely reduced for all widths, as reported by different authors [30]. In this work the reduction is even more pronounced, as a consequence of the wire length: most of the  $J_c$  values are reduced by one order of magnitude. Moreover, devices with the same geometry are affected by a spread of  $J_c$  values bigger than 75%. This spread implies the presence of local damages randomly distributed: the requested degree of homogeneity between parallel stripes belonging to each block is difficult to achieve, and it will therefore degrade the photoresponse. By

considering instead YBCO/LSMO nanowires, we can notice that - as a consequence of having a capping LSMO layer during the last etching step - the wire homogeneity is preserved. We have measured a  $J_c$  spread that is always lower than 50% while the  $J_c$  values are reduced maximum by a factor of 4.

## 6. Preliminary photoresponse measurements

Photo-response experiments have been carried out mounting the devices in a liquid helium flow cryostat with optical access. Electrical connections are given by wire bonds to high bandwidth and low bandwidth cables going to room temperature. The low bandwidth connections are used to dc bias the devices, while the output signals are carried by the high bandwidth connection to two cascaded 1 GHz bandwidth amplifiers with an overall voltage gain of 400.

A voltage response is measured on both YBCO and YBCO/LSMO superconducting nanodevices, when they are biased close to their critical current  $I_c$  and they are illuminated by optical laser pulses at 1550 nm wavelength, as shown in Fig. 4. Here, the laser pulses have a rise and fall time of 3 ns, a duration of 500 ns and intensity of about  $50 \text{ nW}/\mu\text{m}^2$ . By varying dead time we see that the photoresponse appears in correspondence with the illumination of the stripes.

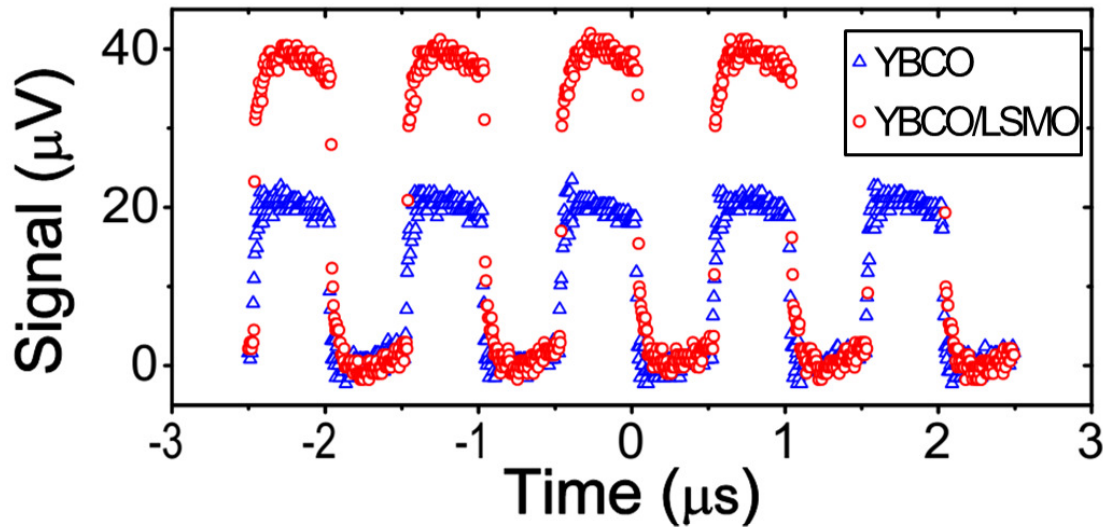


**Figure 4.** Voltage responses measured at 10 K on two devices with the same geometry, but employing respectively bare YBCO and YBCO/LSMO nanowires (wire width = 200 nm). Although the extracted critical current densities of YBCO/LSMO nanowires are almost two orders of magnitude lower than those corresponding to bare YBCO detectors ( $J_c^{YBCO-LSMO} = 7.8 \cdot 10^5 \text{ A/cm}^2$ ,  $J_c^{YBCO} = 1.1 \cdot 10^7 \text{ A/cm}^2$ ), the photoresponse is almost double in amplitude. The bias currents used were  $106 \mu\text{A}$  (for YBCO/LSMO) and  $3340 \mu\text{A}$  (for YBCO), each one close to the respective critical current (0.1 mA and 3.3 mA).

*Highly homogeneous YBCO/LSMO nanowires for photo-response experiments* 8

As can be seen in Fig. 4, the YBCO photoresponse is characterized by a  $\sim 30$  ns rise time and  $\sim 20$  ns fall time, whereas for YBCO/LSMO both rise and fall times were  $\sim 60$  ns. The signal amplitude of YBCO/LSMO is about two times higher than the YBCO signal. This is surprising because the critical current of the bilayer device is much lower than the one of the YBCO device, but it could be due to a higher homogeneity of the bilayer stripes.

However, other mechanisms related to the presence of LSMO as a manganite at the interface with YBCO cannot be excluded. Further analysis of the signals is currently in progress, mainly aimed at understanding the microscopic mechanisms responsible of the observed photo-response.

## 7. Conclusions

In conclusion, we have fabricated YBCO nanowires with a ferromagnetic LSMO capping layer. We have found that the  $T_C$  increases of about 1 K. Furthermore the patterning into nanowires decreases the critical current density almost a factor of 4 for the YBCO/LSMO bilayer and a factor of 10 for bare YBCO. Moreover, the spread in the critical current density was measured to be 75% for YBCO and always lower than 50% for YBCO/LSMO. The transparency of LSMO to optical photons, together with the good degree of homogeneity we have achieved, even for lengths of several microns, allow the implementation of these nanowires in complex configurations, suitable for photodetection experiments. First results in optical illumination have shown that the YBCO/LSMO devices respond in similar way to that of YBCO stripes. The origin of the enhanced response of the YBCO/LSMO bilayers compared to bare YBCO detectors is still to be clarified.

## Acknowledgements

This work has been partially supported by the Swedish Research Council (VR) and the Knut and Alice Wallenberg Foundation. Riccardo Arpaia was partially supported by a grant from the Foundation BLANCEFLOR Boncompagni Ludovisi, née Bildt.

## References

- [1] Gol'tsman G N, Okunev O, Chulkova G, Lipatov A, Semenov A, Smirnov K, Voronov B, Dzardanov A, Williams C and Sobolewski R 2001 *Appl. Phys. Lett.* **79** 705–707
- [2] Natarajan C M, Tanner M G and Hadfield R H 2012 *Supercond. Sci. Technol.* **25** 063001
- [3] Dorenbos S N, Reiger E M, Perinetti U, Zwiller V, Zijlstra T and Klapwijk T M 2008 *Appl. Phys. Lett.* **93** 131101
- [4] Marsili F, Verma V B, Stern J A, Harrington S, Lita A E, Gerrits T, Vayshenker I, Baek B, Shaw M D, Mirin R P and W N S 2013 *Nature Photonics* **7** 210–214
- [5] Shibata H, Takesue H, Honjo T, Akazaki T and Tokura Y 2010 *Appl. Phys. Lett.* **97** 212504
- [6] Curtz N, Koller E, Zbinden H, Decroux M, Antognazza L, Fischer and Gisin N 2010 *Supercond. Sci. Technol.* **23** 045015



*Highly homogeneous YBCO/LSMO nanowires for photo-response experiments* 9

- [7] Larsson P, Nilsson B and Ivanov Z G 2000 *J. Vac. Sci. Technol. B* **18** 25–31
- [8] Assink H, Harg A, Schep C M, Chen N Y, Marel D, Hadley P, Drift E and Mooij J E 1993 *IEEE Trans. Appl. Supercond.* **3** 2983–2985
- [9] Nawaz S, Bauch T and Lombardi F 2011 *IEEE Trans. Appl. Supercond.* **21** 164–167
- [10] Tafuri F, Massarotti D, Galletti L, Stornaiuolo D, Montemurro D, Longobardi L, Lucignano P, Rotoli G, Pepe G, Tagliacozzo A and Lombardi F 2013 *J. Supercond. Nov. Magn.* **26** 21–41
- [11] Nawaz S, Arpaia R, Bauch T and Lombardi F 2013 *Physica C* **495** 33 – 38
- [12] Nawaz S, Arpaia R, Lombardi F and Bauch T 2013 *Phys. Rev. Lett.* **110**(16) 167004
- [13] Przyslupski P, Komissarov I, Paszkowicz W, Dluzewski P, Minikayev R and Sawicki M 2004 *Phys. Rev. B* **69**(13) 134428
- [14] T Petrisor J, Gabor M S, Tiusan C, Galluzzi V, Celentano G, Popa S, Boule A and Petrisor T 2012 *J. Appl. Phys.* **112** 053919
- [15] Parlato L, Arpaia R, De Lisio C, Miletto Granozio F, Pepe G P, Perna P, Pagliarulo V, Bonavolontà C, Radovic M, Wang Y, Sobolewski R and Scotti di Uccio U 2013 *Phys. Rev. B* **87**(13) 134514
- [16] Buzdin A I 2005 *Rev. Mod. Phys.* **77**(3) 935 – 976
- [17] Marrocco N, Pepe G P, Capretti A, Parlato L, Pagliarulo V, Peluso G, Barone A, Cristiano R, Ejrnaes M, Casaburi A, Kashiwazaki N, Taino T, Myoren H and Sobolewski R 2010 *Appl. Phys. Lett.* **97** 092504
- [18] Peña V, Sefrioui Z, Arias D, Leon C, Santamaria J, Varela M, Pennycook S J and Martinez J L 2004 *Phys. Rev. B* **69**(22) 224502
- [19] Yunoki S, Moreo A, Dagotto E, Okamoto S, Kancharla S S and Fujimori A 2007 *Phys. Rev. B* **76**(6) 064532
- [20] Chakhalian J, Freeland J W, Srajer G, Stremper J, Khaliullin G, Cezar J C, Charlton T, Dalgliesh R, Bernhard C, Cristiani G, Habermeier H U and Keimer B 2006 *Nat. Phys.* **2** 244 – 248
- [21] Asulin I, Yuli O, Koren G and Millo O 2006 *Phys. Rev. B* **74**(9) 092501
- [22] Soltan S, Albrecht J and Habermeier H U 2004 *Phys. Rev. B* **70**(14) 144517
- [23] Chen C, Li Y and Cai C 2012 *Solid State Commun.* **152** 1203 – 1207
- [24] Ki S and Dho J 2010 *J. Korean Phys. Soc.* **57**(6) 1879
- [25] Arpaia R, Nawaz S, Lombardi F and Bauch T 2013 *IEEE Trans. Appl. Supercond.* **23** 1101505
- [26] Ejrnaes M, Casaburi A, Quaranta O, Marchetti S, Gaggero A, Mattioli F, Leoni R, Pagano S and Cristiano R 2009 *Supercond. Sci. Technol.* **22** 055006
- [27] Ejrnaes M, Cristiano R, Quaranta O, Pagano S, Gaggero A, Mattioli F, Leoni R, Voronov B and Gol'tsman G 2007 *Appl. Phys. Lett.* **91** 262509
- [28] Verevkin A, Zhang J, Sobolewski R, Lipatov A, Okunev O, Chulkova G, Korneev A, Smirnov K, Gol'tsman G N and Semenov A 2002 *Appl. Phys. Lett.* **80** 4687–4689
- [29] Aytug T, Paranthaman M, Kang B W, Sathyamurthy S, Goyal A and Christen D K 2001 *Appl. Phys. Lett.* **79** 2205–2207
- [30] Papari G, Carillo F, Stornaiuolo D, Longobardi L, Beltram F and Tafuri F 2012 *Supercond. Sci. Technol.* **25** 035011